Plant Biotechnology Journal
Open Access

Plant Biotechnology Journal (2023) **21**, pp. 317–330 doi: 10.1111/pbi.13943

Engineering triacylglycerol accumulation in duckweed (*Lemna japonica*)

Yuanxue Liang[1], Xiao-Hong Yu[1], Sanket Anaokar[1], Hai Shi[1], William B. Dahl[2], Yingqi Cai[1], Guangbin Luo[3], Jin Chai[1], Yuanheng Cai[1], Almudena Mollá-Morales[2], Fredy Altpeter[3], Evan Ernst[2,4], Jorg Schwender[1], Robert A. Martienssen[2,4] and John Shanklin[1,*]

[1]*Biology Department, Brookhaven National Laboratory, Upton, NY, USA*
[2]*Cold Spring Harbor Laboratory, Cold Spring Harbor, NY, USA*
[3]*Agronomy Department, Genetics Institute, University of Florida, Gainesville, FL, USA*
[4]*Howard Hughes Medical Institute, Cold Spring Harbor Laboratory, Cold Spring Harbor, NY, USA*

Received 16 June 2022;
revised 8 September 2022;
accepted 30 September 2022.
**Correspondence* (Tel (631) 344-3414; fax (631) 344-3407; email shanklin@bnl.gov)

Summary

Duckweeds are amongst the fastest growing of higher plants, making them attractive high-biomass targets for biofuel feedstock production. Their fronds have high rates of fatty acid synthesis to meet the demand for new membranes, but triacylglycerols (TAG) only accumulate to very low levels. Here we report on the engineering of *Lemna japonica* for the synthesis and accumulation of TAG in its fronds. This was achieved by expression of an estradiol-inducible cyan fluorescent protein-*Arabidopsis WRINKLED1* fusion protein (*CFP-AtWRI1*), strong constitutive expression of a mouse diacylglycerol:acyl-CoA acyltransferase2 (*MmDGAT*), and a sesame oleosin variant (*SiOLE(*)*). Individual expression of each gene increased TAG accumulation by 1- to 7-fold relative to controls, while expression of pairs of these genes increased TAG by 7- to 45-fold. In uninduced transgenics containing all three genes, TAG accumulation increased by 45-fold to 3.6% of dry weight (DW) without severely impacting growth, and by 108-fold to 8.7% of DW after incubation on medium containing 100 μM estradiol for 4 days. TAG accumulation was accompanied by an increase in total fatty acids of up to three-fold to approximately 15% of DW. Lipid droplets from fronds of all transgenic lines were visible by confocal microscopy of BODIPY-stained fronds. At a conservative 12 tonnes (dry matter) per acre and 10% (DW) TAG, duckweed could produce 350 gallons of oil/acre/year, approximately seven-fold the yield of soybean, and similar to that of oil palm. These findings provide the foundation for optimizing TAG accumulation in duckweed and present a new opportunity for producing biofuels and lipidic bioproducts.

Keywords: duckweed, *Lemna minor*, *WRI1*, *DGAT*, triacylglycerol, plant oil.

Introduction

Lemnaceae, also known as duckweeds, are a family of aquatic monocotyledonous plants with 36 species recognized in five genera (*Spirodela*, *Landoltia*, *Lemna*, *Wolffiella*, and *Wolffia*; Acosta *et al*., 2021; Bog *et al*., 2019, 2020). Duckweeds are the smallest and fastest-growing aquatic flowering plants (Les *et al*., 2002; Wang *et al*., 2010) with doubling time varying between 16 h and 3 days under optimal conditions (Leng *et al*., 1995; Rusoff *et al*., 1980). Their aquatic habit means their growth doesn't displace arable land for conventional crop growth. Robust growth in diverse environments makes duckweeds promising platforms for engineering the accumulation of biofuel and bioproduct feedstocks (Xu *et al*., 2012b).

The availability of high-quality genome information is foundational for genetic and metabolic engineering strategies. In recent years, genome assemblies have been published for *Spirodela polyrhiza* (Michael *et al*., 2020; Wang *et al*., 2014), *Lemna minor* (Van Hoeck *et al*., 2015), *Wolffia australiana* (Michael *et al*., 2020) and *Landoltia punctata* (Hoang *et al*., 2019). Of the five duckweed genera, a full genome is so far missing only for *Wolffiella*, for which the estimated genome size is between ~600 Mb and 1914 Mb (Hoang *et al*., 2019; Wang *et al*., 2011). An important online resource that includes the complete sequence of *L. japonica* is also publicly available (Ernst and Martienssen, 2011). In addition to reliable genome information, efficient stable transformation protocols are needed for the generation of transgenic lines. Protocols based on *Agrobacterium*-mediated transformation of callus cultures have been reported for multiple duckweed species (Boehm *et al*., 2001; Geng *et al*., 2018; Vunsh *et al*., 2007; Wang *et al*., 2021; Yamamoto *et al*., 2001), but the transformation of *L. japonica* clone 8627 is the most efficient by far, so we chose this species in these studies (Cantó-Pastor *et al*., 2015). This clone was previously misclassified as *L. minor* (Braglia *et al*., 2021). Besides the overexpression of foreign genes, the ability to suppress native duckweed genes is also needed. An artificial miRNA approach has been successfully used (Cantó-Pastor *et al*., 2015), as well as CRISPR/Cas9-mediated genome editing (Liu *et al*., 2019b). Transformation of *L. japonica* can be achieved within 5–6 weeks with better than 90% efficiency (Cantó-Pastor *et al*., 2015).

Triacylglycerol (TAG) has more than twice the energy density of starch. For most biomass crops vegetative tissues comprise a major proportion of the total plant biomass, so the accumulation of TAG in plant vegetative tissues is an appealing strategy to produce high yields of TAG for biofuel uses (Xu *et al*., 2020; Yee *et al*., 2021). In duckweeds, almost all the plant biomass is comprised of photosynthetically active tissue in floating leaf-like

fronds, which if genetically modified could potentially produce TAG at high yields per unit land area. A widely used approach to engineer TAG accumulation in vegetative tissues is the so-called push-, pull- and protect approach (Vanhercke *et al*., 2014), which refers to the expression of different factors in combination to increase the flux of metabolic precursors to fatty acid biosynthesis (push), increased enzyme capacity to incorporate fatty acids into TAG (pull) and to minimize degradation of TAG from lipid droplets (protect). Accordingly, increased flux into fatty acid synthesis can be achieved by overexpression of WRINKLED1 (WRI1), a transcription factor of the family of APETALA2/ethylene-responsive element binding proteins, and a well-stablished master transcriptional activator of fatty acid synthesis (Focks and Benning, 1998; Liu *et al*., 2019a; Zhai *et al*., 2017). The heterologous expression of *WRI1* homologs from a variety of species has been shown to induce TAG accumulation (Grimberg *et al*., 2015; Yang *et al*., 2015). Expression of WRI1 in combination with various other genes was shown to synergistically promote oil synthesis and accumulation (An and Suh, 2015; Beechey-Gradwell *et al*., 2019; Lee *et al*., 2017; Vanhercke *et al*., 2013, 2019; Zale *et al*., 2016). The incorporation of fatty acids into TAG can be facilitated by the expression of diacylglycerol acyltransferase (DGAT), which catalyzes the transfer of an acyl group from acyl-CoA to diacylglycerol (Cases *et al*., 1998). The expression of DGAT with an engineered plant structural protein (cysteine [Cys]-oleosin) was shown to result in TAG accumulation in *Arabidopsis* (Winichayakul *et al*., 2013). Suppression of lipid degradation can be achieved by overexpression of *OLEOSIN* (OLE), a structural protein that coats oil bodies in developing seeds and other tissues (Board *et al*., 2022; Chapman *et al*., 2012). In combination, overexpression of *Arabidopsis WRINKLED1* (*AtWRI1*), *Arabidopsis DGAT1* (*AtDGAT1*), and sesame *OLEOSIN1* (*SiOLE*) have resulted in levels of TAG up to 15% of DW in tobacco leaves (Vanhercke *et al*., 2017).

Here we report on two rounds of the design-build-test-learn approach for the engineering of elevated TAG levels in *L. japonica*. For this purpose, we created a series of constructs to express improved push-, pull- and protect factors and expressed them in different combinations. Concerning the push factor *WRINKLED1* (W), we observed morphological changes and reduced growth rate when expressed constitutively. We addressed previously reported protein stability issues and adverse effects of WRI1 expression described herein and elsewhere (Yang *et al*., 2015) in leaf tissues by creating a fusion of AtWRI1 with Cyan Fluorescent Protein (CFP) and by controlling expression via an estradiol inducible promoter. The other two factors, a highly active form of DGAT from mouse, *MmDGAT* (D), and a modified *OLEOSIN* from *Sesame indicum* (*SiOLE(*)*) (O) were constitutively expressed. We characterized stable transformed lines containing W, D, or O individually, binary combinations thereof and with all three genes. In combination, TAG levels were increased from 0.08% of DW in the parental wild type (WT) to a mean of 8.7% across several transgenic lines. Our best line accumulated up to 10% (DW) of TAG resulting from synergistic effects of expression of W, D and O.

Results

Optimization of gene expression in *Lemna japonica*

SiOLE was used to test whether the *ZmHSP70* intron could enhance its expression. A modified *OLEOSIN* from *Sesame indicum* (*Cys-OLEOSIN*) with the *ZmHSP70 intron* (*SiOLE(*)*) or lacking the intron (*SiOLE(S)*) were transiently expressed in *Nicotiana benthamiana* leaves. The *SiOLE(*)* construct significantly increased TAG content to 0.53% by dry weight (DW) in *N. benthamiana* leaves relative to 0.34% by DW for *SiOLE(S)* (Figure 1a). We also assessed the overexpression of maize *ZmWRI1b* driven by the constitutive 35S long (Cauliflower Mosaic Virus) promoter. Separation of extracted lipids by thin layer chromatography (TLC) showed two transgenic lines (ZmWRI1b-1 and ZmWRI1b-2) accumulated 5- to 8-fold more TAG than WT and controls in which enhanced green fluorescence protein (GFP) was overexpressed alone (Figure 1b). Constitutive overexpression of *ZmWRI1b* severely affected duckweed morphology and slowed their growth (Figure 1c). Consistent with our findings, constitutive expression of WRI1 in monocots has been demonstrated to result in negative physiological effects (Yang *et al*., 2015), and reduced biomass accumulation (Parajuli *et al*., 2020). Using what we learned from these experiments, we initiated a second round of the design-build-test-learn cycle making several modifications to our approach. To alleviate issues related to the constitutive expression of *WRI1*, we switched to inducible expression by the estrogen receptor-based XVE system (Schlücking *et al*., 2013). We previously demonstrated that fusing *GFP* to the N-terminus of the Arabidopsis *WRI1* (*GFP-WRI1*) enhanced its stability when expressed in tobacco leaves (Zhai *et al*., 2017), to further improve *AtWRI1* expression, the *Anemonia majano CFP* was codon optimized for *L. japonica* and N-terminally fused to *AtWRI1* (*CFP-AtWRI1*). Since AtWRI1 is localized to the nucleus (Zhai *et al*., 2017), we used confocal microscopy to examine an OW (25-1) line four days after estradiol induction to determine if the optimized CFP-AtWRI1 correctly localized to the nucleus (Figure 1d). The CFP fluorescence (purple arrow) from OW (25-1) fronds colocalizes with the free enhanced YFP (EYFP) fluorescence marker protein diffused into the nucleus, demonstrating that the optimized CFP-AtWRI1 expressed successfully and targets correctly.

Generation of single, double and triple combination transformants of *SiOLE(*)*, *CFP-AtWRI1* and *MmDGAT*

Except for the above-mentioned *CFP-AtWRI1* under the control of the XVE system to avoid the adverse effects of *AtWRI1*, Mouse (*Mus musculus*) *DGAT2* (*MmDGAT*) was used because it is the major metabolic route to TAG accumulation in mouse (Chitraju *et al*., 2019; Smith *et al*., 2000; Stone *et al*., 2004) and we previously reported transient overexpression of the *MmDGAT2* in tobacco leaves resulted in significant TAG accumulation (Cai *et al*., 2019). *SiOLE(*)* was also created to mitigate the breakdown of TAG from lipid droplets (Hamada *et al*., 2020; Hsiao and Tzen, 2011; Lin *et al*., 2002; Tai *et al*., 2001). An overview of all constructs used in this study is shown in Figure 2. We used Golden Gate assembly (Engler *et al*., 2014; Weber *et al*., 2011) to make level one (L1) and level two (L2) constructs (Figure 2) which were used for transformation. An "empty vector" containing *BAR* and *EYFP* L2-0 (EV) was used as a negative control. Constructs or duckweed transgenic lines for single genes for *SiOLE(*)*, *CFP-AtWRI1* and *MmDGAT* were designated as L2-6 (O), L2-22 (W) and L2-24 (D), respectively. Similarly, binary combinations were named L2-25 (OW), L2-27 (OD), and L2-31 (WD). Finally, the three-gene combination was named L2-33 (OWD). All transgenic lines were labeled by their individual line designation as shown in Figure 2. Constructs harboring combinations of *SiOLE(*)*, *CFP-AtWRI1* and *MmDGAT* were transformed into the callus of WT *L. japonica* by *Agrobacterium*-mediated transformation. After selection with

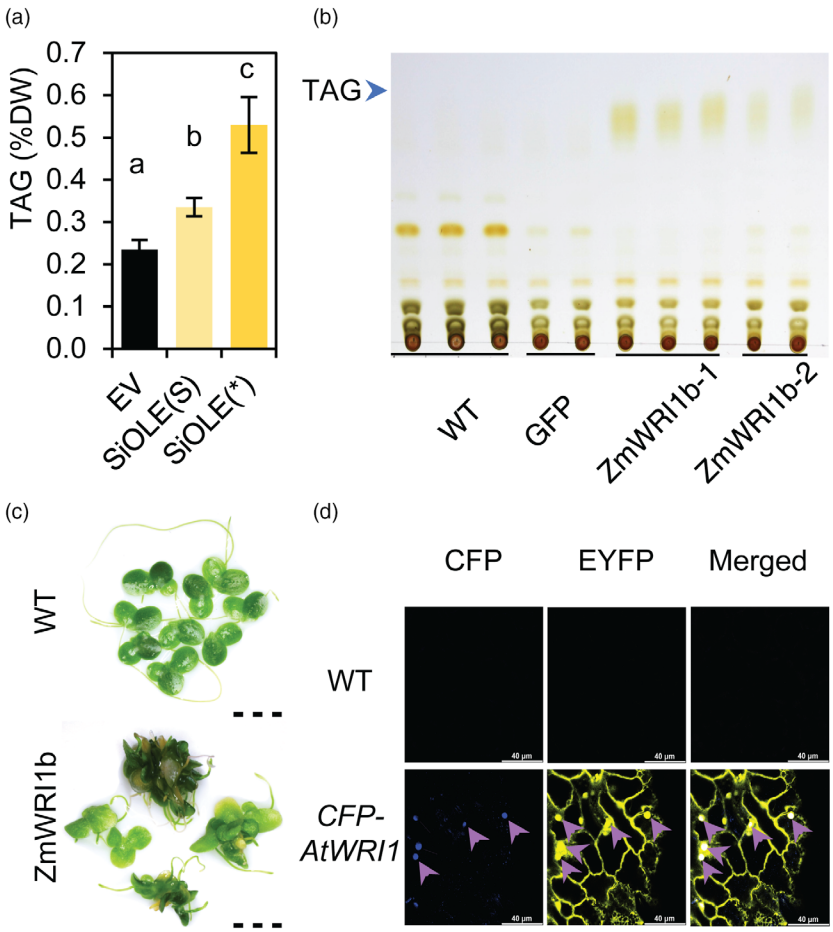

Figure 1 Optimization of gene expression in *Lemna japonica*. (a) Triacylglycerols (TAG) contents in *Nicotiana benthamiana* leaves transiently expressing the modified *SiOLE* with *ZmHSP70* intron (*SiOLE(*)*). (b) Thin layer chromatography (TLC) of lipid from two different P_{35SL}:ZmWRI1b transgenic lines and its parental WT and control line (GFP). (c) Morphology of WT and representative ZmWRI1b overexpression plants. Scale bar = 5 mm. (d) Expression and subcellular localization of AtWRI1 with the optimized *Anemonia majano* Cyan Fluorescent Protein (CFP) fused to the N terminus were assessed by the fluorescence signal of CFP. The CFP fluorescence is shown in blue color and the enhanced YFP (EYFP) is shown in yellow color. The overlapping regions of CFP and EYFP are indicated by purple arrows. Scale bar = 40 μm. Abbreviations: *EV*, empty vector (L2-0); *SiOLE(*)*, sesame *OLEOSIN* with intron (L2-6); WT, Wild type; *ZmHSP70*, maize heat shock protein gene. Data are means of three biological replicates and error bars indicate standard deviations. Significant differences between groups ($P < 0.05$) as identified by one-way ANOVA and Tukey's multiple comparisons test are shown by different letters.

phosphinothricin (PPT), we further screened PPT-resistant lines for EYFP fluorescence using a microplate reader to eliminate false positive lines (Cantó-Pastor *et al.*, 2015). Similar areas of fronds were used for this analysis as shown in Figure S1. The EYFP fluorescence intensities of PPT-resistant lines are shown by a color gradient blue-white-red (133–530–20 000 A.U.; Figure S2a). We obtained 6, 5, 7,4, 4, 3, 2 and 5 positive transgenic lines from EV, O, W, D, OW, OD, WD and OWD constructs, respectively (Figure S2b).

Induction of expression of *CFP-AtWRI1* by estradiol

To induce TAG accumulation in *L. japonica* fronds, only transgenic lines containing *CFP-AtWRI1* and the WT negative control (WT+E) were subject to estradiol induction before quantitative lipid analysis. In this pilot experiment, a 5-day time course of induction with increasing concentrations of estradiol was performed on the OWD line (33-6). TAG content increased from 2.8% of DW of uninduced samples to a maximum of 8.5% of DW upon estradiol induction (Figure S3). Different estradiol concentrations i.e., 50, 100 and 200 μM for 3, 4 or 5 days resulted in similar levels of TAG accumulation, and 100 μM estradiol treatment for 4 days resulted in the highest TAG accumulation (Figure S3). For subsequent experiments, 4-day inductions with 100 μM estradiol were used for two independent representative *CFP-AtWRI1* containing transgenic lines per construct as shown in Figure 3.

Overexpression of *SiOLE(*)*, *CFP-AtWRI1* and *MmDGAT* significantly increases total fatty acid contents and TAG accumulation in *L. japonica* fronds

The effects of single and combinations of *SiOLE(*)*, *CFP-AtWRI1* (4 days induction) and *MmDGAT* on the level of total fatty acids (TFA) are shown in Figure 3a. Untransformed and EV-transformed *L. japonica* (0-5, 0-6) accumulated ~5.4% and ~4.5% of DW of TFA, respectively, and overexpression of OD (27-2 and 27-4), WD (31-1 and 31-3) and OWD (33-5 and 33-6) substantially increased TFA content to 10%, 8% and 15%, respectively (Figure 3a). In control experiments, incubation of WT in media containing

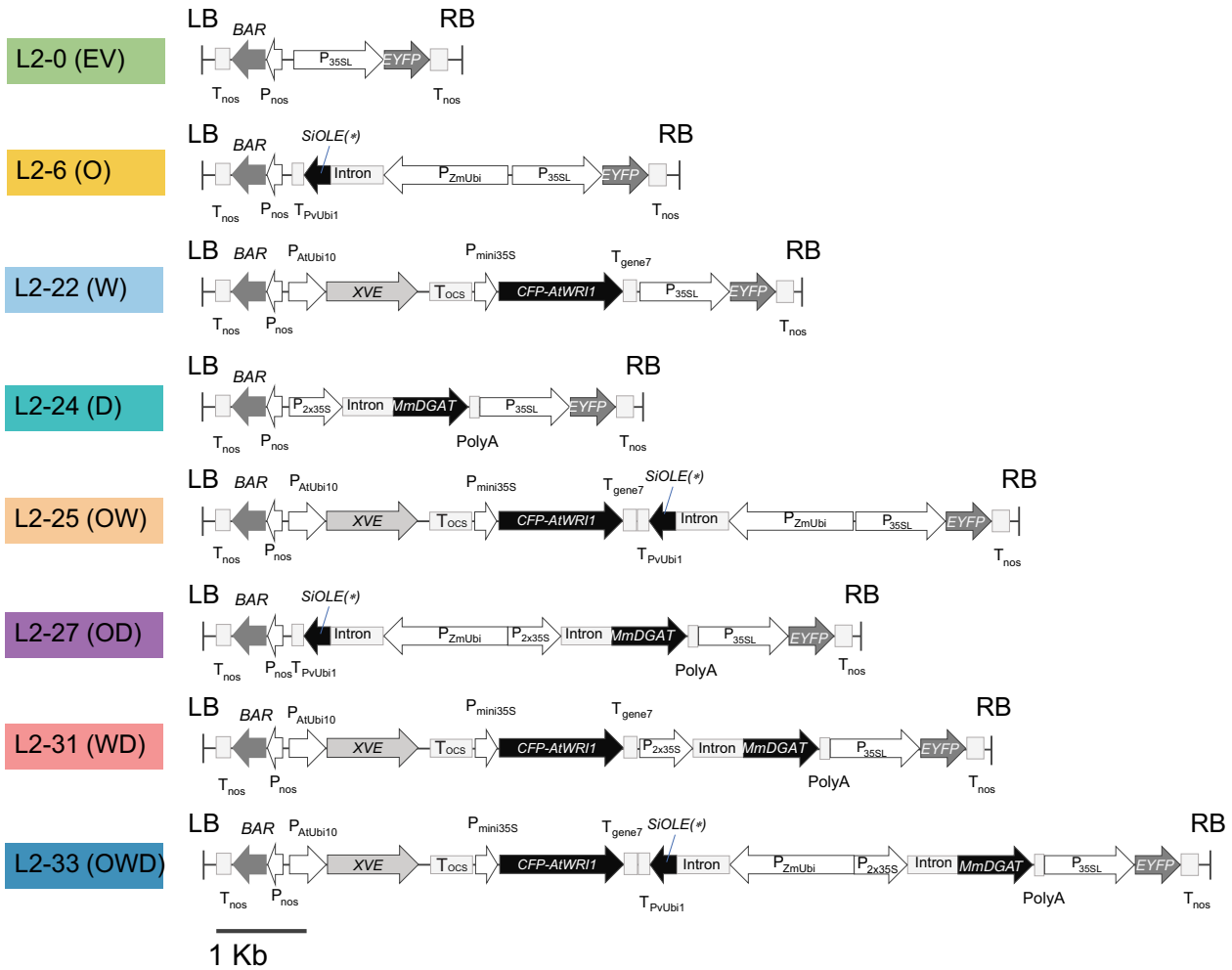

Figure 2 Schematic of the gene constructs with different combinations of *SiOLE(*)*, *CFP-AtWRI1* and *MmDGAT2*. *AtWRI1* with an codon optimized N-terminal cyan fluorescent protein (CFP) fusion under the control of the *XVE* estradiol-inducible promoter, *MmDGAT2* under the strong constitutive 35S promoter and a modified sesame *OLEOSIN (SiOLE(*))* under the control of the strong ZmUbi promoter. The *BAR* and *EYFP* genes which were used for transformants screening were driven by *Agrobacterium tumefaciens* Nos promoter and a long version of 35S promoter (35SL), respectively. The level two L2-0 construct containing only *BAR* and *EYFP* was used as empty vector (EV) control. Scale bar = 1 kb. Abbreviations: At, *A. thaliana*; *BAR*, phosphinothricin acetyl transferase; D, *MmDGAT2*; *EYFP*, Enhanced yellow fluorescent protein; LB, left border; Mm, *M. musculus*; O, *SiOLE(*)*; OD, *SiOLE(*)+MmDGAT2*; OW, *SiOLE(*)+CFP-AtWRI1*; OWD, *SiOLE(*)+CFP-AtWRI1+MmDGAT2*; P, promoter; Pv, *Panicum virgatum*; RB, right border; Si, *S. indicum*; T, Terminator; W, *CFP-AtWRI1*; WD, *CFP-AtWRI1+MmDGAT2*; Zm, *Z. mays*.

100 μM of estradiol (WT+E) did not result in any changes in TFA content.

The effects of single gene expression of *SiOLE(*)*, *CFP-AtWRI1* or *MmDGAT* on TAG accumulation is shown in Figure 3b. Except for O (6-1 and 6-5), the *CFP-AtWRI1* or *MmDGAT*- expressing lines showed a significant approximately 7-fold increase from 0.08% TAG in the parental WT or EV lines to approximately 0.6% for D (24-2) and W (22-4; Figure 3b) lines. Similar increases were observed in the previous design cycle for the 35SL::ZmWRI1b lines described above. The overexpression of two-gene combinations of *SiOLE(*)*, *CFP-AtWRI1* and *MmDGAT* dramatically increased TAG accumulation by 45-fold to approximately 3.6% for OD (27-2, 27-4), by 25-fold to approximately 2% for WD (31-1, 31-3), and by 7-fold to approximately 0.6% of TAG for OW (25-1, 25-3) relative to parental WT or EV controls (Figure 3b).

In addition to comparing TFA or TAG levels of transgenic lines to WT or EV controls, the same data can also be analyzed to assess synergistic effects. We define synergy as when the effect of combined gene expression exceeds the sum of their effects when expressed singly. With respect to the TFA contents (Figure 3a) there were no such effects visible, but synergistic effects were seen for TAG contents (Figure 3b and Table S1). A detailed analysis of six synergy cases with statistical evaluation is shown in Table 1. For example, the sum of the averages in TAG levels for the O-, W- and D lines in Figure 3b, respectively, minus the contributions of the EV control shown in Figure 3b, amounts to 0.93 (%DW). The average TAG level for the two OWD lines in Figure 3b without EV effects is 7.76% (DW), which is 8.4 times higher than the combined levels of the single transformants (*t*-test, $P = 4.0 \times 10^{-15}$, Table 1). The synergy effects are similarly strong and highly significant when comparing the OW and D TAG levels to OWD (8.7 times higher TAG level in OWD), and for comparing O and D to OD (8.8 times higher, Table 1). Other cases that combine W with O, D or OD are less synergistic (with increases of 2.4-fold or less, Table 1), while combining W and O has merely additive effects (0.94, Table 1). These observations

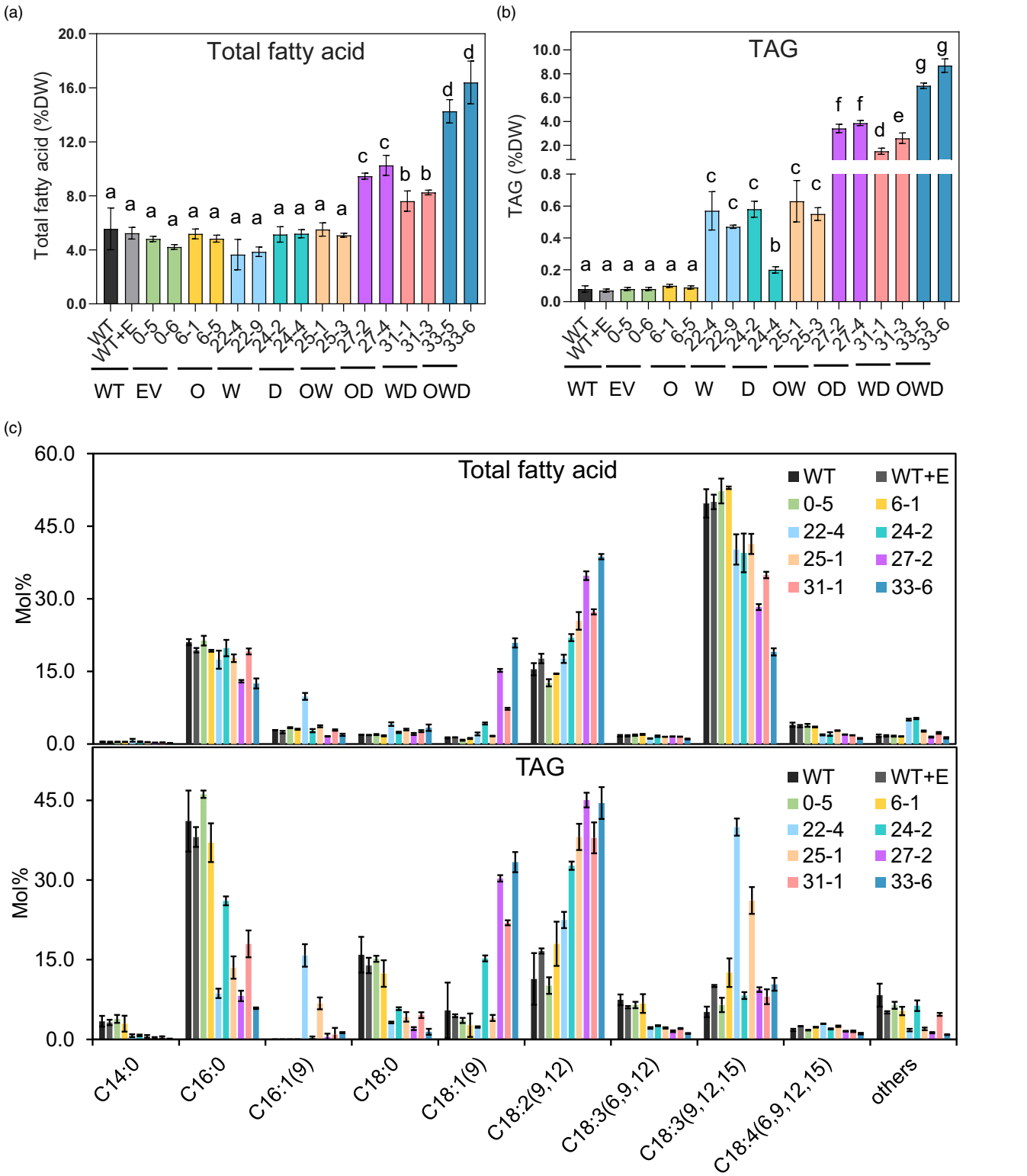

Figure 3 Lipids content and composition. (a) Total fatty acid content by percentage of Dry Weight (DW). (b) Triacylglycerols (TAG) content by percentage of Dry Weight (DW). (c) lipid profiles of total fatty acid and TAG in different transgenic lines. Two representative lines are show in (a) and (b), single representative lines are show in (c). Fronds were cultivated under half-strength SH medium and continuous light approximate 100 μmol m^{-2} s^{-1} cool white fluorescent light illumination at pH 5.6 and at 23 °C with ambient CO_2 level. Data are means of three biological replicates and error bars indicate standard deviations. Significant differences between groups ($P < 0.05$) as identified by one-way ANOVA and Tukey's multiple comparisons test are shown by different letters. Abbreviations: E, Estradiol; WT, *Lj8627* Wild type.

together suggest that the strongest synergy effect arises from combinations that bring O and D together. A similar observation is that among the four assessed combinatorial expressions cases (OW, OD, WD, OWD) the combinations OWD and OD have the highest and second highest measured levels, respectively, both in TFA (Figure 3a) and in TAG (Figure 3b).

To visualize lipid droplets, fronds from each transgenic line were stained with boron-dipyrromethene (BODIPY) and imaged using confocal microscopy. Transgenic lines for the W and D single gene expression showed increased amounts of BODIPY-stained lipid droplets compared to O and the negative controls (Figure 4). The transgenic lines for two-gene combinations (OD, OW, WD) showed enhanced accumulation of lipid droplets relative to the genes expressed singly and controls and the OWD lines showed the strongest signal. These findings are consistent with the TAG data shown in Figure 3b. The lipid droplets were relatively small for lines expressing single genes compared to those expressing two or three of the transgenes. The OD and OWD lines have large oil droplets, but the OWD line has more of them.

Transgenic lines show distinct changes in fatty acid profiles

Since heterologous expression of lipogenic genes can alter fatty acid profiles, we determined the profiles of each representative line (Figure 3c). WT and EV lines mainly accumulate C18:3 (9,12,15) which accounts for around 50% of TFA, whereas, OD, WD and OWD lines accumulate C18:1(9) and C18:2(9,12) with percentages ranging from 7% (WD (31-1)) to 39% (OWD (33-6)) at the expense of C18:3(9,12,15). Analysis of TAG fatty acid profiles showed that C16:0 is present at about 40% in the WT, while it amounts to only 8%, 17% and 6%, respectively in the OD, WD and OWD lines. OD, WD and OWD accumulate 30%, 23% and 31% of C18:1(9), and 45%, 38% and 43% of C18:2 (9,12), respectively.

Several gene combinations containing *WRI1* had an inhibitory effect on growth rate

In preparation for experimental treatments, lines were cultivated in half-strength Schenk & Hildebrandt (SH) medium with a 16-h photoperiod followed by a 3-day exposure to continuous light. The growth curves were generated by daily measurement of frond areas for 10 days of culture under continuous light (Figure 5a) and the corresponding growth rates are presented in Figure 5b. While the OW (25-1 and 25-3) and WD (31-3) lines were found to grow significantly slower than WT and EV lines, the average growth over 10 days of all other lines showed no significant differences from WT or EV (0-5). Thus, it might suggest that even background expression of WRI1 can cause growth inhibition, but this is only the case for OW and WD (31-3), not for W and OWD. Also, since for WD the growth inhibition effect is not consistent (31-1 vs. 31-3), we currently cannot make clear conclusions as to the possible effects of WRI1 expression on growth rates. Besides growth rates, morphological effects were also observed. After 10 days the transgenic lines appeared similar to that of WT and EV. However, the fronds of one WD line (31-3) had a longer frond axis, which gave the appearance of a larger separation between mother and daughter fronds, and the fronds were more triangular-shaped relative to the more rounded WT fronds (Figure 5c). We also observed that the daughter fronds of OWD (33-6) have a yellowish tinge compared to the greener colored WT fronds (Figure 5c).

SiOLE(*), *CFP-AtWRI1* and MmDGAT transcript levels

RT-qPCR was performed to determine the normalized relative transcript levels of the transgenes (Figure 6a–c). The expression level of *MmDGAT* in lines singly expressing *MmDGAT* was similar to that when *MmDGAT* was co-expressed with *SiOLE(*)* and/or *CFP-AtWRI1*. However, the accumulation of *SiOLE(*)* transcript was lower when expressed alone than when expressed with *MmDGAT* or *CFP-AtWRI1*. Conversely, the expression of *CFP-AtWRI1* induced by estradiol was higher when expressed alone than when expressed with *MmDGAT* or *SiOLE(*)*. The protein abundance of CFP-AtWRI1 in different transgenic lines as determined by Western blot was consistent with its transcriptional expression pattern (Figure 6d). While it is unclear why expression of DGAT or OLEOSIN might be somehow attenuating WRI1 expression, this observation is consistent with the above synergy findings, confirming that combining W with O, D or OD has less synergistic effect than combinations that bring O and D together (Table 1).

Discussion

This study demonstrates that duckweed can accumulate significant levels of TFA and TAG as evidenced by the *L. japonica 8627* transgenic line OWD (33-6) which accumulated up to approximately 16% of TFA and 8.7% of TAG on a DW basis. This represents an increase of more than two orders of magnitude of TAG upon the co-expression of the push, pull and protect factors

Table 1 Tests for synergy effects for genes expressed separately and in different combinations

	Genotype/condition						
Separate genotypes	O+W	O+D	W+D	OW+D	OD+W	WD+O	O+W+D
Sum of average TAG levels (S1)*	0.54	0.40	0.83	0.90	4.08	2.06	0.93
Combined expression	OW	OD	WD	OWD	OWD	OWD	OWD
Average TAG level (S2)*	0.51	3.55	1.96	7.76	7.76	7.76	7.76
Ratio S2/S1	0.94	8.79	2.36	8.65	1.90	3.77	8.35
T	−0.93	−18.99	−4.16	−16.53	−8.62	−11.72	−16.79
df	20	20	20	20	20	20	25
P-value	3.6E-01	2.9E-14	4.8E-04	4.0E-13	3.6E-08	2.0E-10	4.0E-15

Mean values (TAG(%DW)) derived from Table S1. For computation of test statistic *T* and *P*-values see Methods.

*Minus the contribution of the empty vector control in each case (Table S1).

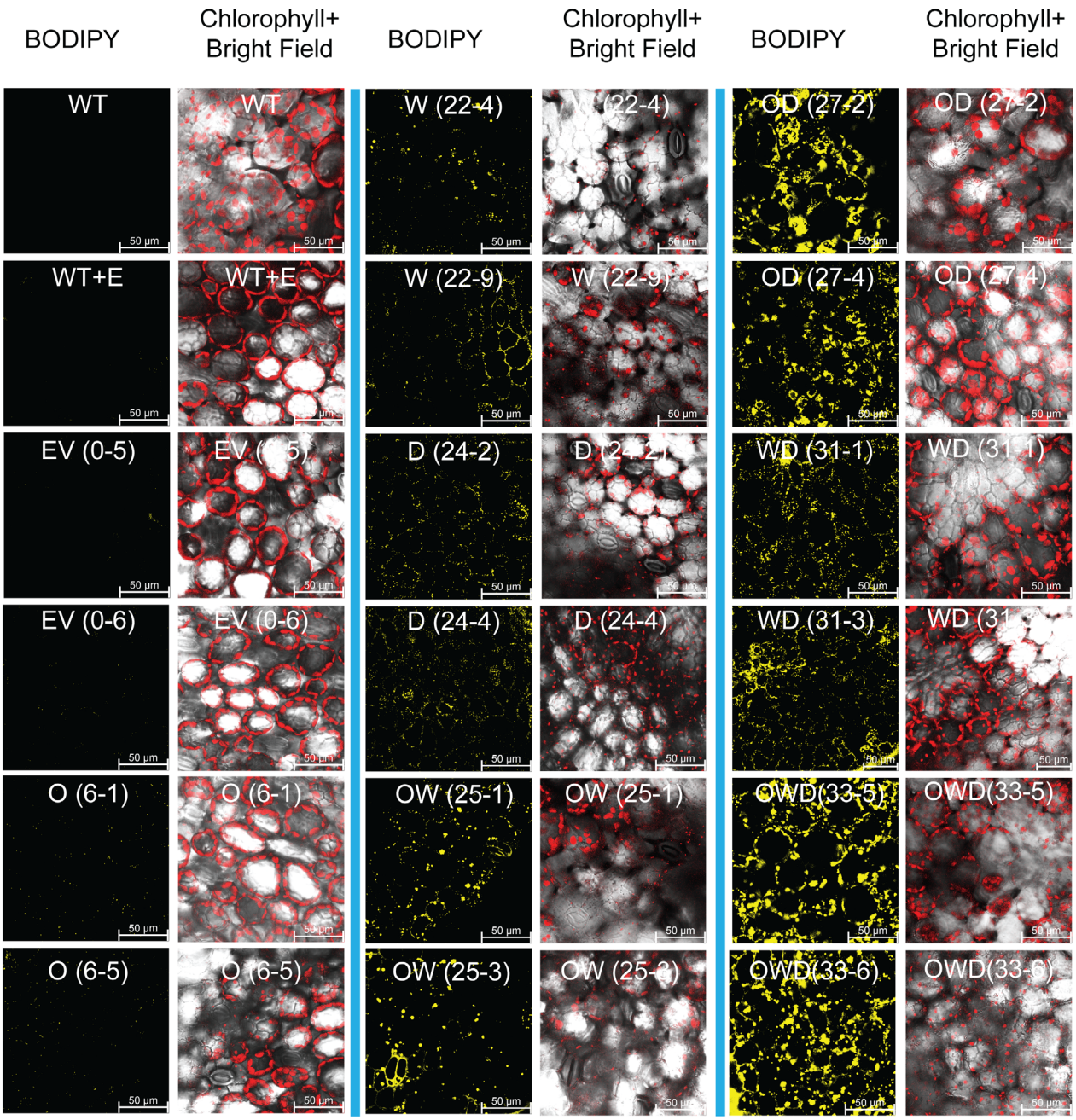

Figure 4 Confocal images of all transgenic lines and WT. Lipid droplets in all lines were shown at left-side of each group with yellow color representing BODIPY signal. The right-side images of each group represent the merged signal of chlorophyll autofluorescence (colored in red) and bright field. Two independent transgenic lines were shown for each gene combination. EV (0-5, 0-6), single gene construct O (6-1, 6-5), W (22-4, 22-9) and D (24-2, 24-4), two gene combination constructs OW (25-1, 25-3), OD (27-2, 27-4), and WD (31-1, 31-3), and three gene combination construct OWD (33-5, 33-6). Scale bar = 50 µm. Abbreviations: D, *MmDGAT*; E, Estradiol; EV, empty vector; O, modified *SiOLE*; W, *CFP-AtWRI1*; WT, *Lj8627* Wild type.

CFP-AtWRI1, *MmDGAT* and *SiOLE(*)* in the fronds relative to the untransformed parental WT *L. japonica*. The stability of line OWD (33-6) is evidenced by the accumulation of equivalent levels of TAG in Figure S3 and Figure 3, which were separated by 7 months and more than 80 generations. In contrast to the three-gene overexpression, the expression of single, W, D, and O genes did not significantly elevate TFA accumulation compared to the untransformed WT or the EV control. However, the co-expression of W and D, and of D and O, respectively, resulted in significant increases in both TFA and TAG, relative to the effect of their expression individually. In contrast, the combination of W and O did not result in a significant increase in TFA relative to their expression individually. Combining W and O did also not result in a significant increase in TAG relative to W alone. In light of the push, pull and protect paradigm this indicates that consecutive factors (push and pull, W and D; pull and protect, D and O) act strongly together while push and protect factors (W, O) do not. Evaluating our data for synergy, i.e., quantifying whether the effect of coexpression is more than the sum of effects of individual expression, we find strong synergy effects in TAG

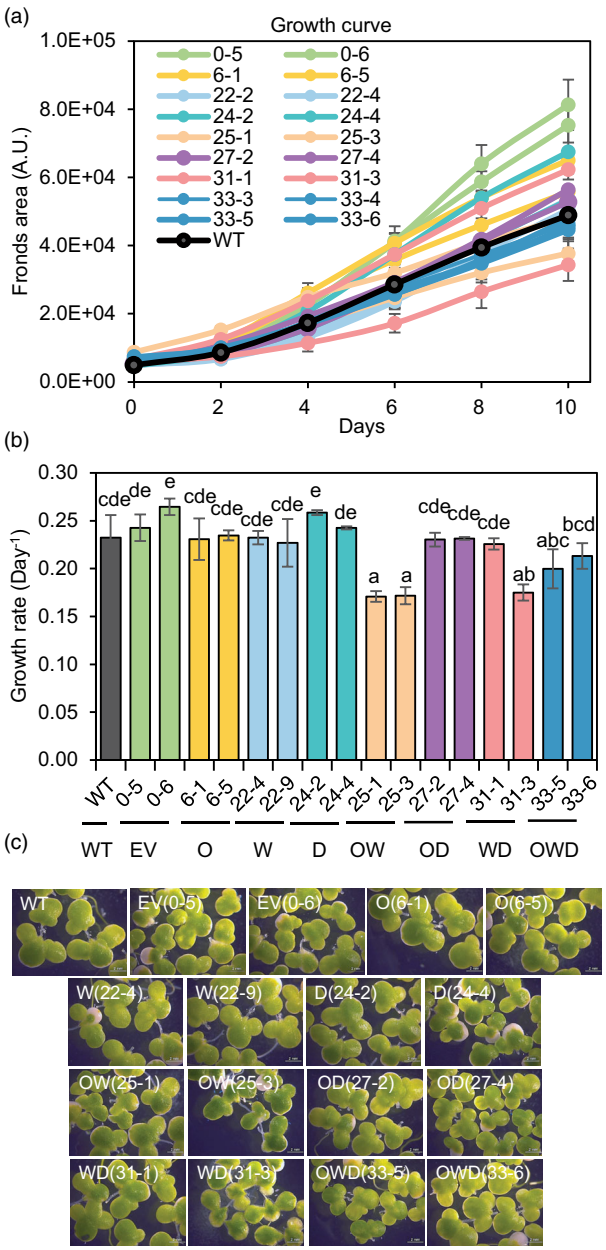

Figure 5 Growth kinetics and morphology. (a) Photoautotrophic growth. (b) Average photoautotrophic growth rate. (c) Morphology comparison. Scale bar = 2 mm. The black line represents WT growth kinetic, and the two green lines show EV (0-5, 0-6) control lines growth, and other curves are for other transgenic lines as indicated in the graph. Fronds were cultivated in half-strength SH medium (pH 5.6) under continuous cool white fluorescent light illumination (approximate 100 μmol m^{-2} s^{-1}) at 23 °C with ambient CO_2 level. Data are means of three biological replicates and error bars indicate standard deviations. Significant differences between groups ($P < 0.05$) as identified by one-way ANOVA and Tukey's multiple comparisons test are shown by different letters.

accumulation when combining O, W and D, when combining OW and D as well as combining O and D. We further find that combining W and O has no synergy effect. Thus, at least the effectiveness of combining O, W and D and the small effect of combining W and O is consistently found. The latter finding implies that the increased FA synthesis resulting from the expression of the push factor W exceeds the capacity of WT DGAT to transfer FA to TAG. The push, pull and protect paradigm assumes that increased TAG accumulation is accomplished through an increased flux through *de-novo* FA synthesis. However, we cannot exclude that TAG is made by the rebalancing of FA chains between membranes and TAG. In cases of expression of O, W and D as well as for coexpression of O and W the TAG levels are well below 1% of DW while in the WT and EV control cases the total FA content ranges between about 4 and 5% of DW. Thus, within uncertainties of experimental error, an undetectable but substantial redistribution of FA from existing membranes to TAG is also possible.

We note that sources for the push-, pull- and protect factors used in these studies and the promoters employed to drive the expression of these genes were chosen somewhat arbitrarily, and it is likely that screening of additional genes encoding each factor for ones that outperform those used in this study in subsequent design-build-test-learn cycles will yield further increases in TAG accumulation. It is also possible that the use of other developmental or tissue-specific promoters for D and O may result in increases in TAG accumulation. Likewise, for the conditional expression of W to avoid the toxic effects of WRI1 expression by a strong constitutive promoter in monocots (Yang *et al*., 2015), we chose to drive *WRI1* with the estradiol inducible XVE promoter system (Schlücking *et al*., 2013; Zuo *et al*., 2000). The use of this system enabled us to successfully obtain and regenerate *AtWRI1* transgenic duckweed from callus culture that lacks the morphological changes and reduced growth rates associated with constitutive expression of WRI1. In XVE-controlled W-expressing lines we observed high *CFP-AtWRI1* transcript levels after 3 days of estradiol induction, and some chlorosis and cell death after 5 days. It is interesting to note that for unknown reasons levels of W transcripts in lines expressing only W, were 5- to 10-fold higher than that in lines co-expressing of O, D, or O and D (Figure 6c,d). However, we note that TFA and TAG levels were much higher in lines in which W was coexpressed with D, or O and D, relative to lines in which W was expressed alone, demonstrating that high levels of W were not necessary for maximal oil accumulation in *L. japonica*. While useful for these pilot studies, the use of an estradiol-inducible promoter may be undesirable for large-scale production because of potential toxicity to humans.

TAG levels of 30% of DW have been reported for tobacco (*Nicotiana tabacum*) leaves (Vanhercke *et al*., 2017), raising the possibility that similar levels could be achieved in duckweed. Further engineering to achieve higher levels could involve additional genetic manipulation. That WT *L. japonica* typically accumulates only 0.08% TAG (DW) is consistent with it having a high capacity for lipid degradation and that downregulation of TAG lipases such as SDP1 (Kelly *et al*., 2013) could result in a doubling of TAG accumulation levels as previously reported for tobacco (Vanhercke *et al*., 2017). Successful achievement of such levels would result in duckweed biomass having approximately 50% higher TAG than that of soybeans, currently the world's largest source of vegetable oil. In terms of yield per acre per year, soybeans produce approximately 55 gal of oil. Duckweed yields in the southern USA can reach 20 tonnes per acre per year (Leng *et al*., 1995), which at 10% of its DW as oil, would potentially yield 720 gal of oil, i.e., approximately 13-fold the yield of soybean. This is more than four times that was reported by Vanhercke *et al*. (2019) for the best transgenic sorghum lines and similar to that of oil palm. If production lines of duckweed can be further optimized to produce 20% TAG (DW), the theoretical oil

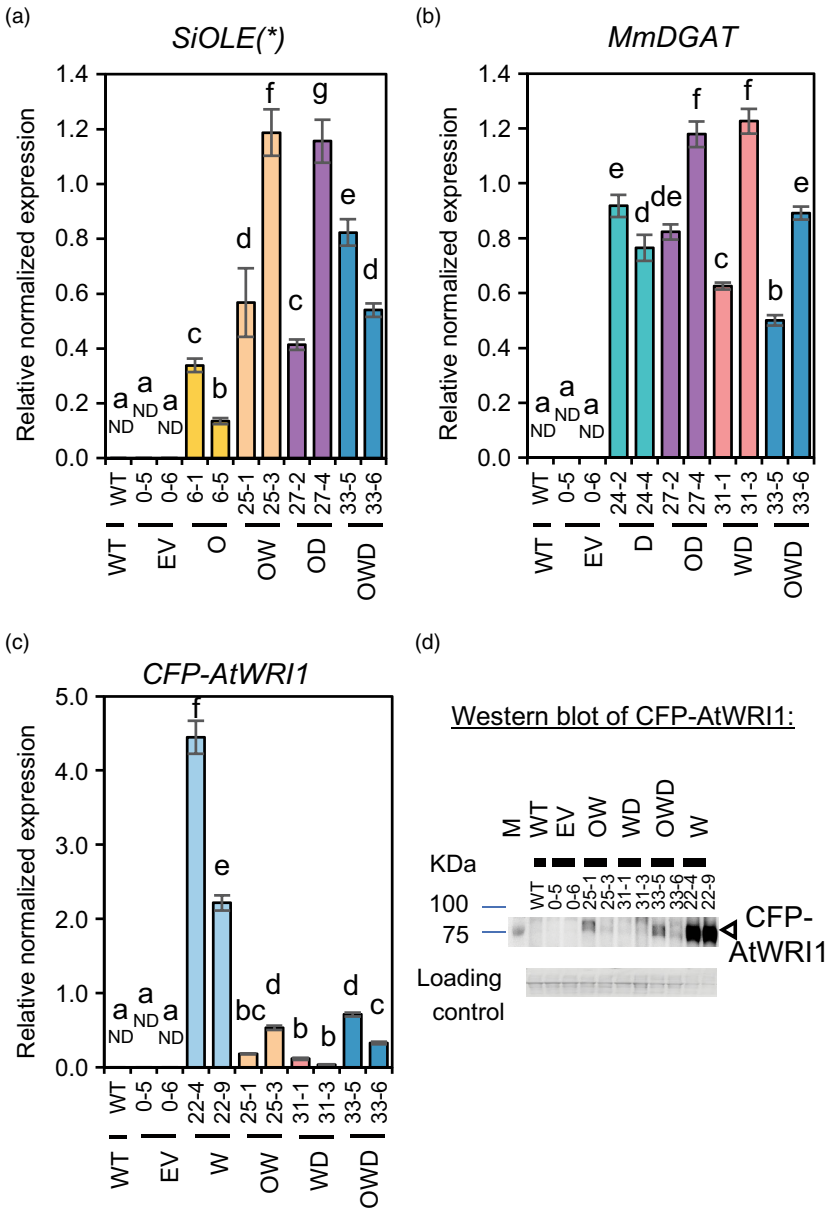

Figure 6 Quantitative RT-PCR analysis of transcriptional expression of *SiOLE(*)* (a), *MmDGAT* (b) and *CFP-AtWRI1* (c) in different transgenic lines, as well as the Western blot result of CFP-AtWRI1 (d). Fronds were cultivated in half-strength SH medium (pH 5.6) under continuous cool white fluorescent light illumination (approximate 100 μmol m^{-2} s^{-1}) at 23 °C with ambient CO_2 level. Data are means of three biological replicates and error bars indicate standard deviations. Significant differences between groups ($P < 0.05$) as identified by one-way ANOVA and Tukey's multiple comparisons test are shown by different letters.

yield could reach 1440 gal per acre per year, i.e., it could exceed that of soybean by approximately 25-fold. The ability of duckweeds to obtain nutrients from agricultural waste streams that normally pollute the environment, adds to their attractiveness as sources of biofuel feedstocks (Xu *et al.*, 2012a; Ziegler *et al.*, 2016).

Besides the accumulation of TFA and TAG, the rate at which the transgenic lines grow is of interest. With a constitutive expression of O and D and background expression of W, a significant reduction in growth was found (Figure 5b). Several recent studies aimed at engineering TAG accumulation in vegetative tissues of various plants reported reduced growth or yield penalty effects (Chu *et al.*, 2020; Mitchell *et al.*, 2020; Parajuli *et al.*, 2020; Vanhercke *et al.*, 2017). Among various possible explanations are: (i) Limitations in the supply of energy cofactors and carbon precursors under conditions of resource diversion to TAG synthesis at high rates. (ii) Energy drain caused by high rates of TAG synthesis and degradation (futile cycling). (iii) Pathway imbalances under high rates of fatty acid and TAG synthesis – for example build-up of free fatty acids to toxic levels (Yang *et al.*, 2015). (iv) Interference of TAG accumulation with the maintenance of the composition and quantity of cellular membranes. (v) Besides the known gene targets of WRI1 associated with the conversion of carbohydrates into fatty acids, there might be interference of this transcription factor with other processes that could have negative effects. These questions are

currently being investigated and it is noteworthy that the lower morphological complexity of duckweed compared to other higher plants, the precision with which physiological conditions can be controlled and growth rates determined, makes *Lemna japonica* well suited for future studies of this phenomenon.

The FA composition of WT duckweed consists mainly of C18:3, C16:0 and C18:2 (Chakrabarti *et al*., 2018; Sharma *et al*., 2019; Tang *et al*., 2015; Yan *et al*., 2013). In contrast, oil-accumulating transgenic lines show an increase of unsaturated FA, including C16:1(9), C18:1(9), C18:2(9,12) and C18:3(9,12,15) in their TAG, and a decrease in C18:3(9,12,15) in their TFA, consistent with a large proportion of their C18:1 or C18:2 being packaged into TAG reducing the availability of C18:2 for further desaturated to C18:3. This trend was strongest in higher TAG accumulation lines, such as in OD, WD and OWD, suggesting TAG biosynthesis is outcompeting polar lipid synthesis for mono- and di-unsaturated FA due in part to the substrate preference of MmDGAT. The resulting reduction in C18:3(9,12,15) in cellular membranes likely contributes to the chlorotic phenotype in the days following the induction of lipid synthesis.

The final committed step in TAG synthesis is the DGAT-mediated conversion of diacylglycerol (DAG) to TAG. DGATs from different species have distinct activities when heterologously expressed. The MmDGAT from an animal source has a relative high activity in plants compared to other those plant DGATs (Cai *et al*., 2019). The successful expression of animal enzymes in plants has been reported a number of times, for example, the expression of fish docosahexaenoic acid (DHA) and eicosapentaenoic acid (EPA) biosynthetic enzymes show similar levels of activity in plants (Venegas-Caleron *et al*., 2010). To date there are few examples of animal-sourced enzymes used to engineer plant metabolism and whether they can be useful in boosting plant lipid synthesis (Cai *et al*., 2017). In screening plant and mouse DGATs for their efficacy in plant lipid accumulation, we found the MmDGAT to outperform the tested plant-sourced enzymes. While this may appear counter intuitive, cross-kingdom heterologous expression of enzymes can be a useful way of avoiding regulatory feedback mechanisms that are specific to a particular kingdom as previously demonstrated (Stark *et al*., 1992). Alternatively, some enzymes may have evolved higher rates of catalysis to meet the metabolic demands of their natural hosts. Further study will be needed to determine why MmDGAT is so efficient when expressed in plants.

While work from our group to increase the transformation efficiency of *L. japonica* was successful (Cantó-Pastor *et al*., 2015), the problem of long-term storage of both WT and transgenic lines remains to be solved. This is because while duckweeds are flowering plants, robust methodologies to induce flowering and harvest seeds have yet to be reported. Thus, subculturing and maintenance at reduced temperatures is currently the best option. Biocontainment of transgenic duckweed is an important concern for the industrial production of high-oil duckweed. It is envisaged that a system employing a "kill switch" analogous to those previously described (Chan *et al*., 2016) could be developed to mitigate this issue.

Methods

Materials and callus induction

A duckweed strain, *Lemna japonica* 8627 used in this study was originally obtained from the Rutgers Duckweed Stock cooperative of Rutgers University. The duckweed was cultivated in SH-modified medium (Schenk and Hildebrandt, 1972) with 1% (w/v) sucrose (SHS), pH5.6 (plantMedia, Dublin, OH, USA) for 2–3 weeks under 100 μmol m^{-2} s^{-1} light illumination in a 16-h photoperiod and at 23 °C. Calli were induced by incubating duckweed fronds on induction medium (IM; Cantó-Pastor *et al*., 2015). Briefly, 4.4 g/L Murashige and Skoog (MS) basal salts (Murashige and Skoog, 1962) plus 3% (w/v) sucrose, with 5 μM 2,4-dichlorophenoxyacetic acid (2,4-D) and 0.5 μM thidiazuron (TDZ) was used as IM, pH5.6. After one month, the fastest growing calli were propagated in nodule production medium (NPM), containing 4.4 g/L MS basal salts, 3% (w/v) sucrose, 10 mM 2,4-D and 20 mM 6-benzylaminopurine (BAP).

Codon optimization of cyan fluorescence protein (CFP)

A *CFP* gene from *Anemonia majano* with relatively narrow excitation and emission spectra was codon optimized based on a 60% GC content for expression in *L. japonica* (Figure S4). To further improve gene expression, a 10 bp Kozak sequence (CTCGAGGCCG; Kozak, 1987, 1989) from the *Spirodela polyrhiza WRI1* gene (Asrani *et al*., 2018) was fused to the start codon of *CFP*.

Vector construction

The ZmWRI1b coding sequence along with UTR regions was amplified from ZmWRI1b plasmid cloned into the pB7WG2D Gateway destination vector behind the 35SL promoter.

To enhance the expression level of *MmDGAT* and *SiOLE(*)*, an intron from the maize 70 KDa heat shock protein 1_8 (ZmHSP70) followed by a Kozak sequence were introduced upstream of each of the ORFs. To prevent gene silencing in stably transformed lines, different promoters and terminators were used for each of the transgenes. Phosphinothricin acetyl transferase (*BAR*) was used as the selection maker to identify transgenics.

GoldenGate modular cloning components of the MoClo Toolkit (Weber *et al*., 2011; Werner *et al*., 2012) and the MoClo Plant Parts Kit (Engler *et al*., 2014) from *Addgene* (http://www.addgene.org/www.addgene.org) were used for vector constructions. The AGL1 *Agrobacterium* strain and a modified level 2 accept vector (pICSL4723-just-L2) were used for these studies. To clone genes into Golden Gate vectors, we changed those nucleobases in the genes with *BsaI*, *BpiI* or *BsmBI* restriction sites. To combine these different elements, a PCR-based method was used to make two new Level zero acceptor vectors which with TACT-GATG (for 5′ untranslated sequence (5U) part) and GATG-GCTT (for coding sequence 1 (CDS1) part) sticky ends after digestion with *BsaI*. With the concern of WRI1 adverse physiological effects on duckweed, the inducible XVE system (Schlücking *et al*., 2013; Zuo *et al*., 2000) was used, which is regulated by estradiol. An optimized *CFP* with relative narrow excitation and emission spectrum was synthesized by GENEWIZ (https://www.genewiz.com/en) and fused to the N-terminal of *AtWRI1* to get *CFP-AtWRI1*, which was under the control of bacterial LexA operator fused upstream (−46 to +12) of the 35S minimal promoter and *A. tumefaciens* gene7 terminator. The *XVE* fusion gene was driven by *Arabidopsis* ubiquitin 10 promoter ($P_{AtUbi10}$) and with *A. tumefaciens* ocs terminator (T_{OCS}; Figure 2). *MmDGAT* expression was driven by the strong constitutive 2x35S promoter (P_{2x35S}) and terminated by the PolyA signal of 35S (Figure 2). The modified sesame *Cys-OLEOSIN (SiOLE(*))* was driven by the strong maize polyubiquitin 3 promoter (P_{ZmUbi}) and terminated by the switchgrass ubiquitin 1 terminator (T_{PvUbi1}; Figure 2). Different combination of *SiOLE(*)*, *CFP-AtWRI1* and

MmDGAT (Figure 2) were constructed according to the method described (Engler *et al*., 2014; Weber *et al*., 2011; Werner *et al*., 2012). Names and sequences of primers, template plasmid, PCR product length, annealing temperature, DNA ligase, restriction digestion enzymes and antibiotic selection markers are shown in Table S2.

Agrobacterium preparation and transient expression in tobacco (*Nicotiana benthamiana*) leaves

Constructed expression vectors were transformed into *Agrobacterium tumefaciens* AGL1 strain using a BioRad micropulser electroporator. Transformed AGL1 containing, EV, *SiOLE(*) or SiOLE(S)* (Figure 1a) were cultivated in Luria-Bertani (LB) medium with appropriate antibiotics to OD_{600} = 1.0. After centrifugation, cell pellets were resuspended in infiltration buffer containing 10 mM MES, pH5.6, 10 mM $MgCl_2$, and 200 μM acetosyringone (AS) and adjusted to OD_{600} = 0.8. The cells were incubated for 2 h at room temperature with gentle shaking (Norkunas *et al*., 2018), and an equal volume of *Agrobacterium* cells containing *P19* gene (Voinnet *et al*., 2003) was included in each infiltration mixture. The mixture was infiltrated into the leaves of 4-week-old *N. benthamiana* plants. Following infiltration, the plants were left at 28 °C for an hour before returning to the growth chamber (Wood *et al*., 2009).

Duckweed callus transformation

We performed the transformation of duckweed as previously described (Cantó-Pastor *et al*., 2015), for the ZmWRI1b lines, and with minor modifications for the OWD lines. *Agrobacterium tumefaciens* GV3101 (ZmWRI1b) or AGL1 (OWD) cells containing different constructs were cultivated with appropriate antibiotics and 100 μM AS at 28 °C to OD_{600} around 0.8. Then cells were spun down and resuspended in the infection medium (10 mM $MgCl_2$, 1% sucrose and 200 μM AS) and cultured for 2 h. Finally, cells were diluted with infection medium to OD_{600} = 0.2. Calli from *Lemna japonica* were cut into small pieces and immersed in *Agrobacterium* for 5 min, then vacuum infiltrated for 8 min at 34 kPa, followed by 5 min at normal pressure and vacuum for another 8 min. Then, calli were cultivated on NPM medium with 100 μM of AS for 3 days under dark at 23 °C.

Selection and regeneration of transgenic plants

After three days of co-cultivation, the infected calli were transferred onto regeneration and selection medium (Liu *et al*., 2019b). Briefly, Gamborg's B5 basal medium supplemented with 1% sucrose, 4.65 μM kinetin, 2.57 μM indole-3-acetic acid (IAA), 10 mg/L PPT and 400 mg/L timentin were added. Calli were cultured under a 16-h photoperiod of 50 μmol m^{-2} s^{-1} of light. Regenerated fronds were proliferated on SHS liquid medium.

Fluorescence screen of transformed plants

All transformed plants were verified by detecting YFP fluorescence using a TECAN SPARK 20M multimode microplate reader (TECAN US, Durham, NC: Tecan Genios, Grödig, Austria). The excitation wavelength was set at 485 nm with a bandwidth of 20 nm, and the emission wavelength was set at 535 nm with 20 nm of bandwidth.

RNA isolation and cDNA preparation

Total RNA from *L. japonica* was extracted using Direct-zol RNA miniprep kit (Zymo Research Corp, Orange, CA, USA) following the manufacturer's protocol. The first strand cDNA of each line was synthesized from 2 μg of total RNA using the SuperScript IV VILO Master Mix with ezDNase kit (ThermoFisher Scientific, Waltham, MA, USA) following the manufacturer's protocol.

Reverse transcription- quantitative PCR (RT-qPCR)

RT-qPCR was carried out using SsoAdvanced Universal SYBR Green Supermix (Bio-Rad, Hercules, CA, USA) following the instruction from the manufacturer to analyze transgene expression. The *L. japonica* α-tubulin coding gene was used as the reference gene (Cantó-Pastor *et al*., 2015). Primers for qPCR are described in Table S2.

Lipids extraction and analysis by Thin-Layer Chromatography (TLC) and Gas Chromatography-Mass Spectrometry (GC-MS)

For oil extraction, duckweed lines were treated with 100 μM estradiol in half-strength SH medium and continuous light for 4 days, and 100 mg fresh fronds of each line were lyophilized using the dry FreeZone system (Labconco, Kansas City, MO, USA) for 2 days. A total of 800 μL of methanol:chloroform:-formic acid (2:1:0.1, v/v/v) and 20 μg of C17:0 TAG standard were added into each sample followed by shaking for 2 h. Finally, 400 μL of 1 M KCl with 0.2 M phosphoric acid (H_3PO_4) was added. Then centrifuged at 17 000 ***g*** for 5 min, and 30 μL of chloroform phase were used for total fatty acids analysis. For TAG analysis, 75 μL of lipid extract was separated by thin layer chromatography (TLC), and subsequently, the TAG fraction was scraped off and trans-methylated with 1 mL 12% (w/w) boron trichloride (BCl_3) in methanol for 90 min at 85 °C (Zhai *et al*., 2018), except for the ZmWRI1b experiment, 100 μL of total lipid were loaded and development with hexane:diethyl ether:acetic acid (80:20:1, v/v/v) on TLC plate, followed air dried and exposed in iodine vapor. Fatty acid methyl esters (FAMEs) were analyzed on GC-MS with an Agilent J&W DB 23 capillary column (30 m × 0.25 mm × 0.25 μm) as described previously (Yu *et al*., 2014).

Confocal microscopy

Leica TCS SP5 confocal scanning laser microscope was used to detect the fluorescence of the CFP and the EYFP to verify the subcellular localization of CFP-AtWRI1 in duckweed cells. Fluorescent proteins were excited by a laser at 458 nm for CFP and 514 nm for EYFP, and the emission signal was collected between 459–498 nm for CFP and between 563–605 nm for EYFP. To visualize lipid droplets, fronds from different lines were cultivated under continuous light for 4 days (for *CFP-AtWRI1* containing lines 100 μM of estradiol was added), stained with 10 μg/mL BODIPY 493/503 (Invitrogen, Eugene, OR, USA) and imaged using a Leica TCS SP5 laser scanning confocal microscope with excitation at 488 nm and emission at 492–508 nm for BODIPY and 700–784 nm for chlorophyll autofluorescence.

Western blot analysis of CFP-AtWRI1 expression

For immunoblot analysis, total protein was extracted from different lines as described previously (Zhai *et al*., 2017). Generally, proteins were extracted from 2.5 mg fresh weight of each sample and separated by SDS-PAGE using Tris-MOPS-SDS running buffer. Then proteins were transferred to BioTrace NT nitrocellulose membrane and immunoblotted with anti-WRI1 antibodies (1/1000) from rabbit (Zhai *et al*., 2017).

Growth rate analysis of *Lemna japonica* cultures

The growth rate per day (r) was calculated based on the equation from (Naumann *et al*., 2007) for exponential growth:

$$r = \frac{\ln A_t - \ln A_0}{t - t_0},$$

where A_t and A_0 are the frond area at time t and start point (t_0), respectively. We used the time points 0 and 10 days for the calculation.

Statistical analysis of synergistic effects

For statistical analysis of synergistic effects for the expression of W, D and O, we applied a modified t-test as described by (Demidenko and Miller, 2019). For example, for a WD double gene expression event, the null hypothesis is defined as the mean WD TAG content minus the sum of the mean TAG contents of W and D lines, minus the mean TAG content of the empty vector control.

Accession numbers

The GenBank accession number for genes reported in this paper are as follows: *AtWRI1* (AT3G54320), *Cys-OLEOSIN* (AAD42942), *ZmHSP70* (Zm00001d012420), *ZmWRI1b* (GRMZM2G174834), *MmDGAT* (AF384160), *CFP* (AF168421)

Acknowledgements

This work was primarily supported by the U.S. Department of Energy, Office of Science, Office of Biological and Environmental Research program under Award Numbers DE-SC0018244 (Y.L., H.S., W.D., E.E., J.Sc., R.M., J.Sh), and DE-SC0018254 (S.A., Yu.C.), and in part by the DOE Center for Advanced Bioenergy and Bioproducts Innovation (U.S. Department of Energy, Office of Science, Office of Biological and Environmental Research under Award Number DE-SC0018420; Yi.C., G.L., F.A. J. Sh. and X.Y) for providing recombinant DNA vectors and gene constructs that contributed to this work. The Division of Chemical Sciences, Geosciences, and Biosciences, Office of Basic Energy Sciences, US Department of Energy (grant DOE KC0304000; J.C. and J. Sh.) for contributing gene constructs to this work. The confocal microscopic study at the Center for Functional Nanomaterials at Brookhaven National Laboratory was supported under Office of Basic Energy Sciences of DOE with contract no. DE-SC0012704 (to CFN). We thank Dr. Mircea Cotlet and Dr. Changcheng Xu for assistance with confocal microscopy. We also thank Dr. Zhiyang Zhai and Dr. Jantana Keereetaweep for sharing the *GFP-WRI1* gene and the anti-WRI1antibody. We also thank Dr. Peter Rogowsky (Université de Lyon) for sharing the ZmWRI1b plasmid.

Conflicts of interest

The authors declare no conflicts of interest.

Author contributions

J.Sh., Y.L., X.Y., A. M.-M., E.E., R.M., and J.Sc. designed experiments. Y.L. performed experiments, analyzed data and made figures and table with support from X.Y., W.D., X.Y., A. M.-M., and E.E. performed some of the callus induction, transformation and regeneration. S.A., Yi.C., Yu.C., G.L., W.D., A.M.-M and FA contributed to construction of recombinant DNA vectors. H.S. and J.Sc. optimized oil accumulation conditions and analyzed growth rates. S.A., Yi.C., Yu.C., and X.Y. carried out transient overexpression in tobacco. J.C. performed fluorescence screening of transformed plants. Yi.C. helped with confocal microscopy. Y.L. and J.Sh., wrote the article with input from X.Y. S.A. Yi.C., Yu.C., J.Sc., E.E., and R.M. All authors approved the article.

Data availability

All data generated or analyzed during this study are included in this article and in its Supporting Information. Source data are provided with this paper.

References

Acosta, K., Appenroth, K.J., Borisjuk, L., Edelman, M., Heinig, U., Jansen, M.A.K., Oyama, T. *et al*. (2021) Return of the Lemnaceae: duckweed as a model plant system in the genomics and postgenomics era. *Plant Cell*, **33**, 3207–3234.

An, D. and Suh, M.C. (2015) Overexpression of Arabidopsis WRI1 enhanced seed mass and storage oil content in *Camelina sativa*. *Plant Biotechnol. Rep.* **9**, 137–148.

Asrani, K.H., Farelli, J.D., Stahley, M.R., Miller, R.L., Cheng, C.J., Subramanian, R.R. and Brown, J.M. (2018) Optimization of mRNA untranslated regions for improved expression of therapeutic mRNA. *RNA Biol.* **15**, 756–762.

Beechey-Gradwell, Z., Cooney, L., Winichayakul, S., Andrews, M., Hea, S.Y., Crowther, T. and Roberts, N. (2019) Storing carbon in leaf lipid sinks enhances perennial ryegrass carbon capture especially under high N and elevated CO_2. *J. Exp. Bot.* **71**, 2351–2361.

Board, A.J., Crowther, J.M., Acevedo-Fani, A., Meisrimler, C.N., Jameson, G.B. and Dobson, R.C.J. (2022) How plants solubilise seed fats: revisiting oleosin structure and function to inform commercial applications. *Biophys. Rev.* **14**, 257–266.

Boehm, R., Kruse, C., Voeste, D., Barth, S. and Schnabl, H. (2001) A transient transformation system for duckweed (*Wolffia columbiana*) using *Agrobacterium*-mediated gene transfer. *J. Appl. Bot.* **75**, 107–111.

Bog, M., Appenroth, K.-J. and Sree, K.S. (2019) Duckweed (Lemnaceae): its molecular taxonomy. *Front. Sustain. Food Syst.* **3**, 117.

Bog, M., Sree, K.S., Fuchs, J., Hoang, P.T., Schubert, I., Kuever, J., Rabenstein, A. *et al*. (2020) A taxonomic revision of Lemna sect. Uninerves (Lemnaceae). *Taxon*, **69**, 56–66.

Braglia, L., Lauria, M., Appenroth, K.J., Bog, M., Breviario, D., Grasso, A., Gavazzi, F. *et al*. (2021) Duckweed species genotyping and interspecific hybrid discovery by tubulin-based polymorphism fingerprinting. *Front. Plant Sci.* **12**, 270.

Cai, Y., McClinchie, E., Price, A., Nguyen, T.N., Gidda, S.K., Watt, S.C., Yurchenko, O. *et al*. (2017) Mouse fat storage-inducing transmembrane protein 2 (FIT2) promotes lipid droplet accumulation in plants. *Plant Biotechnol. J.* **15**, 824–836.

Cai, Y.Q., Whitehead, P., Chappell, J. and Chapman, K.D. (2019) Mouse lipogenic proteins promote the co-accumulation of triacylglycerols and sesquiterpenes in plant cells. *Planta*, **250**, 79–94.

Cantó-Pastor, A., Mollá-Morales, A., Ernst, E., Dahl, W., Zhai, J., Yan, Y., Meyers, B. *et al*. (2015) Efficient transformation and artificial mi RNA gene silencing in *Lemna minor*. *Plant Biol.* **17**, 59–65.

Cases, S., Smith, S.J., Zheng, Y.-W., Myers, H.M., Lear, S.R., Sande, E., Novak, S. *et al*. (1998) Identification of a gene encoding an acyl CoA:diacylglycerol acyltransferase, a key enzyme in triacylglycerol synthesis. *Proc. Natl Acad. Sci. USA*, **95**, 13018–13023.

Chakrabarti, R., Clark, W.D., Sharma, J.G., Goswami, R.K., Shrivastav, A.K. and Tocher, D.R. (2018) Mass production of *Lemna minor* and its amino acid and fatty acid profiles. *Front. Chem.* **6**, 479.

Chan, C.T.Y., Lee, J.W., Cameron, D.E., Bashor, C.J. and Collins, J.J. (2016) 'Deadman' and 'Passcode' microbial kill switches for bacterial containment. *Nat. Chem. Biol.* **12**, 82–86.

Chapman, K.D., Dyer, J.M. and Mullen, R.T. (2012) Biogenesis and functions of lipid droplets in plants: thematic review series: lipid droplet synthesis and metabolism: from yeast to man. *J. Lipid Res.* **53**, 215–226.

Chitraju, C., Walther, T.C. and Farese, R.V. (2019) The triglyceride synthesis enzymes DGAT1 and DGAT2 have distinct and overlapping functions in adipocytes. *J. Lipid Res.* **60**, 1112–1120.

Chu, K.L., Jenkins, L.M., Bailey, S.R., Kambhampati, S., Koley, S., Foley, K., Arp, J.J., Czymmek, K.J., Bates, P.D. and Allen, D.K. (2020) *Shifting carbon flux from non-transient starch to lipid allows oil accumulation in transgenic tobacco leaves. BioRxiv*.

Demidenko, E. and Miller, T.W. (2019) Statistical determination of synergy based on bliss definition of drugs independence. *PLoS One*, **14**, e0224137.

Engler, C., Youles, M., Gruetzner, R., Ehnert, T.-M., Werner, S., Jones, J.D., Patron, N.J. *et al*. (2014) A golden gate modular cloning toolbox for plants. *ACS Synth. Biol.* **3**, 839–843.

Ernst, E. and Martienssen, R.A. (2011) *Lemna.org - Lemnaceae Genome Repository*. http://www.lemna.org

Focks, N. and Benning, C. (1998) wrinkled1: A novel, low-seed-oil mutant of Arabidopsis with a deficiency in the seed-specific regulation of carbohydrate metabolism. *Plant Physiol.* **118**, 91–101.

Geng, Q.Q., Li, T., Li, P.L., Wang, X., Chu, W.J., Ma, Y.N., Ma, H. *et al*. (2018) The accumulation, transformation, and effects of quinestrol in duckweed (*Spirodela polyrhiza* L.). *Sci. Total Environ.* **634**, 1034–1041.

Grimberg, Å., Carlsson, A.S., Marttila, S., Bhalerao, R. and Hofvander, P. (2015) Transcriptional transitions in *Nicotiana benthamiana* leaves upon induction of oil synthesis by WRINKLED1 homologs from diverse species and tissues. *BMC Plant Biol.* **15**, 1–17.

Hamada, S., Kishikawa, A. and Yoshida, M. (2020) Proteomic analysis of lipid droplets in *Sesamum indicum*. *Protein J.* **39**, 366–376.

Hoang, P.T.N., Schubert, V., Meister, A., Fuchs, J. and Schubert, I. (2019) Variation in genome size, cell and nucleus volume, chromosome number and rDNA loci among duckweeds. *Sci. Rep.* **9**, 13.

Hsiao, E.S.L. and Tzen, J.T.C. (2011) Ubiquitination of oleosin-H and caleosin in sesame oil bodies after seed germination. *Plant Physiol. Biochem.* **49**, 77–81.

Kelly, A.A., van Erp, H., Quettier, A.-L., Shaw, E., Menard, G., Kurup, S. and Eastmond, P.J. (2013) The SUGAR-DEPENDENT1 lipase limits triacylglycerol accumulation in vegetative tissues of Arabidopsis. *Plant Physiol.* **162**, 1282–1289.

Kozak, M. (1987) An analysis of 5′-noncoding sequences from 699 vertebrate messenger RNAs. *Nucleic Acids Res.* **15**, 8125–8148.

Kozak, M. (1989) The scanning model for translation: an update. *J. Cell Biol.* **108**, 229–241.

Lee, K.R., Kim, E.H., Kim, K.H., Park, J.S. and Kim, H.U. (2017) Vegetable oil production in vegetative plant tissues. *Plant Biotechnol. Rep.* **11**, 385–395.

Leng, R., Stambolie, J. and Bell, R. (1995) Duckweed-a potential high-protein feed resource for domestic animals and fish. *Livestock Res. Rural Dev.* **7**, 36.

Les, D.H., Crawford, D.J., Landolt, E., Gabel, J.D. and Kemball, R.T. (2002) Phylogeny and systematics of Lemnaceae, the duckweed family. *Syst. Bot.* **27**, 221–240.

Lin, L.J., Tai, S.S.K., Peng, C.C. and Tzen, J.T.C. (2002) Steroleosin, a sterol-binding dehydrogenase in seed oil bodies. *Plant Physiol.* **128**, 1200–1211.

Liu, H., Zhai, Z., Kuczynski, K., Keereetaweep, J., Schwender, J. and Shanklin, J. (2019a) WRINKLED1 regulates BIOTIN ATTACHMENT DOMAIN-CONTAINING proteins that inhibit fatty acid synthesis. *Plant Physiol.* **181**, 55–62.

Liu, Y., Wang, Y., Xu, S., Tang, X., Zhao, J., Yu, C., He, G. *et al*. (2019b) Efficient genetic transformation and CRISPR/Cas9-mediated genome editing in *Lemna aequinoctialis*. *Plant Biotechnol. J.* **17**, 2143–2152.

Michael, T.P., Ernst, E., Hartwick, N., Chu, P., Bryant, D., Gilbert, S., Ortleb, S. *et al*. (2020) Genome and time-of-day transcriptome of *Wolffia australiana* link morphological minimization with gene loss and less growth control. *Genome Res.* **31**, 225–238.

Mitchell, M.C., Pritchard, J., Okada, S., Zhang, J., Venables, I., Vanhercke, T. and Ral, J.P. (2020) Increasing growth and yield by altering carbon metabolism in a transgenic leaf oil crop. *Plant Biotechnol. J.* **18**, 2042–2052.

Murashige, T. and Skoog, F. (1962) A revised medium for rapid growth and bio assays with tobacco tissue cultures. *Physiol. Plant.* **15**, 473–497.

Naumann, B., Eberius, M. and Appenroth, K.-J. (2007) Growth rate based dose–response relationships and EC-values of ten heavy metals using the duckweed growth inhibition test (ISO 20079) with *Lemna minor* L. clone St. *J. Plant Physiol.* **164**, 1656–1664.

Norkunas, K., Harding, R., Dale, J. and Dugdale, B. (2018) Improving agroinfiltration-based transient gene expression in *Nicotiana benthamiana*. *Plant Methods*, **14**, 1–14.

Parajuli, S., Kannan, B., Karan, R., Sanahuja, G., Liu, H., Garcia-Ruiz, E., Kumar, D. *et al*. (2020) Towards oilcane: engineering hyperaccumulation of triacylglycerol into sugarcane stems. *GCB Bioenergy*, **12**, 476–490.

Rusoff, L.L., Blakeney, E.W., Jr. and Culley, D.D., Jr. (1980) Duckweeds (Lemnaceae family): a potential source of protein and amino acids. *J. Agric. Food Chem.* **28**, 848–850.

Schenk, R.U. and Hildebrandt, A. (1972) Medium and techniques for induction and growth of monocotyledonous and dicotyledonous plant cell cultures. *Can. J. Bot.* **50**, 199–204.

Schlücking, K., Edel, K.H., Köster, P., Drerup, M.M., Eckert, C., Steinhorst, L., Waadt, R. *et al*. (2013) A new β-estradiol-inducible vector set that facilitates easy construction and efficient expression of transgenes reveals CBL3-dependent cytoplasm to tonoplast translocation of CIPK5. *Mol. Plant*, **6**, 1814–1829.

Sharma, J., Clark, W.D., Shrivastav, A.K., Goswami, R.K., Tocher, D.R. and Chakrabarti, R. (2019) Production potential of greater duckweed *Spirodela polyrhiza* (L. Schleiden) and its biochemical composition evaluation. *Aquaculture*, **513**, 734419.

Smith, S.J., Cases, S., Jensen, D.R., Chen, H.C., Sande, E., Tow, B., Sanan, D.A. *et al*. (2000) Obesity resistance and multiple mechanisms of triglyceride synthesis in mice lacking Dgat. *Nat. Genet.* **25**, 87–90.

Stark, D.M., Timmerman, K.P., Barry, G.F., Preiss, J. and Kishore, G.M. (1992) Regulation of the amount of starch in plant tissues by ADP glucose pyrophosphorylase. *Science*, **258**, 287–292.

Stone, S.J., Myers, H.M., Watkins, S.M., Brown, B.E., Feingold, K.R., Elias, P.M. and Farese, R.V., Jr. (2004) Lipopenia and skin barrier abnormalities in DGAT2-deficient mice. *J. Biol. Chem.* **279**, 11767–11776.

Tai, S.S.K., Lee, T.T.T., Tsai, C.C.Y., Yiu, T.J. and Tzen, J.T.C. (2001) Expression pattern and deposition of three storage proteins, 11S globulin, 2S albumin and 7S globulin in maturing sesame seeds. *Plant Physiol. Biochem.* **39**, 981–992.

Tang, J., Li, Y., Ma, J. and Cheng, J.J. (2015) Survey of duckweed diversity in Lake Chao and total fatty acid, triacylglycerol, profiles of representative strains. *Plant Biol.* **17**, 1066–1072.

Van Hoeck, A., Horemans, N., Monsieurs, P., Cao, H.X., Vandenhove, H. and Blust, R. (2015) The first draft genome of the aquatic model plant *Lemna minor* opens the route for future stress physiology research and biotechnological applications. *Biotechnol. Biofuels*, **8**, 188.

Vanhercke, T., El Tahchy, A., Shrestha, P., Zhou, X.R., Singh, S.P. and Petrie, J.R. (2013) Synergistic effect of WRI1 and DGAT1 coexpression on triacylglycerol biosynthesis in plants. *Febs Lett.* **587**, 364–369.

Vanhercke, T., El Tahchy, A., Liu, Q., Zhou, X.R., Shrestha, P., Divi, U.K., Ral, J.P. *et al*. (2014) Metabolic engineering of biomass for high energy density: oilseed-like triacylglycerol yields from plant leaves. *Plant Biotechnol. J.* **12**, 231–239.

Vanhercke, T., Divi, U.K., El Tahchy, A., Liu, Q., Mitchell, M., Taylor, M.C., Eastmond, P.J. *et al*. (2017) Step changes in leaf oil accumulation via iterative metabolic engineering. *Metab. Eng.* **39**, 237–246.

Vanhercke, T., Belide, S., Taylor, M.C., El Tahchy, A., Okada, S., Rolland, V., Liu, Q. *et al*. (2019) Up-regulation of lipid biosynthesis increases the oil content in leaves of Sorghum bicolor. *Plant Biotechnol. J.* **17**, 220–232.

Venegas-Caleron, M., Sayanova, O. and Napier, J.A. (2010) An alternative to fish oils: metabolic engineering of oil-seed crops to produce omega-3 long chain polyunsaturated fatty acids. *Prog. Lipid Res.* **49**, 108–119.

Voinnet, O., Rivas, S., Mestre, P. and Baulcombe, D. (2003) An enhanced transient expression system in plants based on suppression of gene silencing by the p19 protein of tomato bushy stunt virus. *Plant J.* **33**, 949–956.

Vunsh, R., Li, J.H., Hanania, U., Edelman, M., Flaishman, M., Perl, A., Wisniewski, J.P. *et al*. (2007) High expression of transgene protein in *Spirodela*. *Plant Cell Rep.* **26**, 1511–1519.

Wang, W., Wu, Y., Yan, Y., Ermakova, M., Kerstetter, R. and Messing, J. (2010) DNA barcoding of the Lemnaceae, a family of aquatic monocots. *BMC Plant Biol.* **10**, 1–11.

,

Wang, W., Kerstetter, R.A. and Michael, T.P. (2011) Evolution of genome size in duckweeds (Lemnaceae). *J. Bot.* **2011**, 1–9.

Wang, W., Haberer, G., Gundlach, H., Gläßer, C., Nussbaumer, T., Luo, M., Lomsadze, A. *et al*. (2014) The *Spirodela polyrhiza* genome reveals insights into its neotenous reduction fast growth and aquatic lifestyle. *Nat. Commun.* **5**, 1–13.

Wang, K.-T., Hong, M.-C., Wu, Y.-S. and Wu, T.-M. (2021) *Agrobacterium*-mediated genetic transformation of taiwanese isolates of *Lemna aequinoctialis*. *Plants*, **10**, 1576.

Weber, E., Engler, C., Gruetzner, R., Werner, S. and Marillonnet, S. (2011) A modular cloning system for standardized assembly of multigene constructs. *PLoS One*, **6**, e16765.

Werner, S., Engler, C., Weber, E., Gruetzner, R. and Marillonnet, S. (2012) Fast track assembly of multigene constructs using Golden Gate cloning and the MoClo system. *Bioeng. Bugs.* **3**, 38–43.

Winichayakul, S., Scott, R.W., Roldan, M., Hatier, J.-H.B., Livingston, S., Cookson, R., Curran, A.C. *et al*. (2013) In vivo packaging of triacylglycerols enhances Arabidopsis leaf biomass and energy density. *Plant Physiol.* **162**, 626–639.

Wood, C.C., Petrie, J.R., Shrestha, P., Mansour, M.P., Nichols, P.D., Green, A.G. and Singh, S.P. (2009) A leaf-based assay using interchangeable design principles to rapidly assemble multistep recombinant pathways. *Plant Biotechnol. J.* **7**, 914–924.

Xu, J., Cheng, J.J. and Stomp, A.M. (2012a) Growing *Spirodela polyrrhiza* in swine wastewater for the production of animal feed and fuel ethanol: a pilot study. *CLEAN–Soil Air Water*, **40**, 760–765.

Xu, J.L., Zhao, H., Stomp, A.M. and Cheng, J.J. (2012b) The production of duckweed as a source of biofuels. *Biofuels*, **3**, 589–601.

Xu, X.Y., Akbar, S., Shrestha, P., Venugoban, L., Devilla, R., Hussain, D., Lee, J.W. *et al*. (2020) A synergistic genetic engineering strategy induced triacylglycerol accumulation in potato (*Solanum tuberosum*) leaf. *Front. Plant Sci.* **11**, 215.

Yamamoto, Y.T., Rajbhandari, N., Lin, X.H., Bergmann, B.A., Nishimura, Y. and Stomp, A.M. (2001) Genetic transformation of duckweed *Lemna gibba* and *Lemna minor*. *In Vitro Cell. Dev. Biol. Plant*, **37**, 349–353.

Yan, Y., Candreva, J., Shi, H., Ernst, E., Martienssen, R., Schwender, J. and Shanklin, J. (2013) Survey of the total fatty acid and triacylglycerol composition and content of 30 duckweed species and cloning of a Δ6-desaturase responsible for the production of γ-linolenic and stearidonic acids in *Lemna gibba*. *BMC Plant Biol.* **13**, 1–14.

Yang, Y., Munz, J., Cass, C., Zienkiewicz, A., Kong, Q., Ma, W., Sanjaya, S. *et al*. (2015) Ectopic expression of WRINKLED1 affects fatty acid homeostasis in *Brachypodium distachyon* vegetative tissues. *Plant Physiol.* **169**, 1836–1847.

Yee, S., Rolland, V., Reynolds, K.B., Shrestha, P., Ma, L., Singh, S.P., Vanhercke, T. *et al*. (2021) *Sesamum indicum* Oleosin L improves oil packaging in *Nicotiana benthamiana* leaves. *Plant Direct*, **5**, e343.

Yu, X.-H., Prakash, R.R., Sweet, M. and Shanklin, J. (2014) Coexpressing *Escherichia coli* cyclopropane synthase with *Sterculia foetida* lysophosphatidic acid acyltransferase enhances cyclopropane fatty acid accumulation. *Plant Physiol.* **164**, 455–465.

Zale, J., Jung, J.H., Kim, J.Y., Pathak, B., Karan, R., Liu, H., Chen, X.H. *et al*. (2016) Metabolic engineering of sugarcane to accumulate energy-dense triacylglycerols in vegetative biomass. *Plant Biotechnol. J.* **14**, 661–669.

Zhai, Z., Liu, H. and Shanklin, J. (2017) Phosphorylation of WRINKLED1 by KIN10 results in its proteasomal degradation, providing a link between energy homeostasis and lipid biosynthesis. *Plant Cell*, **29**, 871–889.

Zhai, Z., Keereetaweep, J., Liu, H., Feil, R., Lunn, J.E. and Shanklin, J. (2018) Trehalose 6-phosphate positively regulates fatty acid synthesis by stabilizing WRINKLED1. *Plant Cell*, **30**, 2616–2627.

Ziegler, P., Sree, K. and Appenroth, K.-J. (2016) Duckweeds for water remediation and toxicity testing. *Toxicol. Environ. Chem.* **98**, 1127–1154.

Zuo, J., Niu, Q.-W. and Chua, N.-H. (2000) An estrogen receptor-based transactivator XVE mediates highly inducible gene expression in transgenic plants. *Plant J.* **24**, 265–273.

Supporting information

Additional supporting information may be found online in the Supporting Information section at the end of the article.

Figure S1 Representative images of duckweed.
Figure S2 Screening of *L. japonica* transformants using plate reader.
Figure S3 TAG accumulation in duckweed treated with different concentrations of estradiol for different time periods.
Figure S4 Sequence and features of optimized *CFP*.
Table S1 TAG content as percent (DW) in WT and different transgenic lines of *Lemna japonica*.
Table S2 Golden gate clone and qPCR primers.

,